Publication Year	2016
Acceptance in OA	2021-04-15T13:30:02Z
Title	The Gaia spectrophotometric standard stars survey - III. Short-term variability monitoring
Authors	MARINONI, SILVIA, PANCINO, ELENA, ALTAVILLA, GIUSEPPE, BELLAZZINI, Michele, GALLETI, SILVIA, Tessicini, G., Valentini, G., Cocozza, G., Ragaini, S., Braga, Vittorio Francesco, BRAGAGLIA, Angela, Federici, L., Schuster, W. J., Carrasco, J. M., Castro, A., Figueras, F., Jordi, C.
Publisher's version (DOI)	10.1093/mnras/stw1886
Handle	http://hdl.handle.net/20.500.12386/30755
Journal	MONTHLY NOTICES OF THE ROYAL ASTRONOMICAL SOCIETY
Volume	462

Monthly Notices
of the
ROYAL ASTRONOMICAL SOCIETY

MNRAS **462,** 3616–3627 (2016)
Advance Access publication 2016 July 30

doi:10.1093/mnras/stw1886

The *Gaia* spectrophotometric standard stars survey – III. Short-term variability monitoring★

S. Marinoni,[1,2]† E. Pancino,[2,3]† G. Altavilla,[4]† M. Bellazzini,[4] S. Galleti,[4] G. Tessicini,[4] G. Valentini,[5] G. Cocozza,[4] S. Ragaini,[4] V. Braga,[2,6] A. Bragaglia,[4] L. Federici,[4] W. J. Schuster,[7] J. M. Carrasco,[8] A. Castro,[7] F. Figueras[8] and C. Jordi[8]

[1]*INAF-Osservatorio Astronomico di Roma, Via Frascati 33, I-00040, Monte Porzio Catone (Roma), Italy*
[2]*ASI Science Data Center, via del Politecnico SNC, I-00133 Roma, Italy*
[3]*INAF-Osservatorio Astrofisico di Arcetri, largo Enrico Fermi 5, I-50125 Firenze, Italy*
[4]*INAF-Osservatorio Astronomico di Bologna, via Ranzani 1, I-40127 Bologna, Italy*
[5]*INAF-Osservatorio Astronomico di Teramo, via Mentore Maggini SNC, I-64100 Teramo, Italy*
[6]*Department of Physics, Università di Roma Tor Vergata, via della Ricerca Scientifica 1, I-00133 Roma, Italy*
[7]*Observatorio Astronómico Nacional, Universidad Nacional Autónoma de México, Apartado Postal 877, C. P. 22800 Ensenada, B. C., México*
[8]*Departament de Física Quàntica i Astrofísica, Institut del Ciènces del Cosmos (ICC), Universitat de Barcelona (IEEC-UB), c/Martí i Franquès, 1, E-08028 Barcelona, Spain*

Accepted 2016 July 27. Received 2016 July 27; in original form 2016 June 23

ABSTRACT

We present the results of the short-term constancy monitoring of candidate *Gaia* Spectrophotometric Standard Stars (SPSS). We obtained time series of typically 1.24 h – with sampling periods from 1–3 min to a few hours, depending on the case – to monitor the constancy of our candidate SPSS down to 10 mmag, as required for the calibration of *Gaia* photometric data. We monitored 162 out of a total of 212 SPSS candidates. The observing campaign started in 2006 and finished in 2015, using 143 observing nights on nine different instruments covering both hemispheres. Using differential photometry techniques, we built light curves with a typical precision of 4 mmag, depending on the data quality. As a result of our constancy assessment, 150 SPSS candidates were validated against short-term variability, and only 12 were rejected because of variability including some widely used flux standards such as BD+174708, SA 105−448, 1740346, and HD 37725.

Key words: techniques: photometric – binaries: general – stars: variables: general.

1 INTRODUCTION

The *Gaia*[1] satellite (Lindegren & Perryman 1996; Mignard 2005) is a cornerstone mission of the ESA (European Space Agency) Space Programme, launched by a Soyuz-Fregat vehicle in 2013 December 19 from the European Spaceport in Kourou, French Guiana. *Gaia* is performing an all-sky survey to obtain positions, parallaxes and proper motions to μas precision for more than one billion point-like sources on the sky. Expected accuracies are in the 7–25 μas range down to 15th mag and sub-mas accuracies down to a limiting magnitude of $V \simeq 20$ mag. The astrometric data are complemented by low-resolution spectrophotometric data in the 330–1050 nm wavelength range and, for the brightest stars ($V < 16$ mag), by radial velocity measurements in the spectral region centred around the calcium triplet (845–872 nm) at a resolution of about $R = \lambda/\Delta\lambda \simeq 11500$, with 1–15 km s^{-1} errors, depending on spectral type and brightness.

The Astrometric Field CCDs will provide *G*-band images, i.e. white light images where the passband is defined by the telescope optics transmission and the CCD sensitivity, with a very broad combined passband ranging from 330 to 1050 nm and peaking around 500–600 nm. The blue (BP) and red (RP) spectro-photometers will provide dispersed images with $20 < \lambda/\Delta\lambda < 100$ over the spectral ranges 330–680 nm and 640–1050 nm, respectively.

The final conversion of internally calibrated G instrumental magnitudes and BP/RP instrumental fluxes into physical units requires an external absolute flux scale, which our team is in charge of providing (Pancino et al. 2012). Ideally, the *Gaia* spectrophotometric standard stars (SPSS) grid should comprise the order of 200 SPSS in the range $9 \leq V \leq 15$ mag, properly distributed in the sky to be

★Based on data obtained within the *Gaia* DPAC (Data Processing and Analysis Consortium) – and coordinated by the GBOG (Ground-based Observations for *Gaia*) working group – at various telescopes (see acknowledgements).

†E-mail: silvia.marinoni@asdc.asi.it (SM); pancino@arcetri.inaf.it (EP); giuseppe.altavilla@oabo.inaf.it (GA)

[1] http://www.cosmos.esa.int/web/gaia/home

© 2016 The Authors
Published by Oxford University Press on behalf of the Royal Astronomical Society

Downloaded from https://academic.oup.com/mnras/article/462/4/3616/2589704 by guest on 09 April 2021

Table 1. Observation diary of the constancy monitoring campaign. The columns contain: (1) the instrument used; (2) the telescope; (3) the observing site; (4) the campaign time-span; (5) the number of nights awarded to the short-term monitoring campaigns (within brackets the number of useful nights); (6) the number of observed time series; (7) the number of monitored SPSS.

Instrument	Telescope	Site	Period	No. of (useful) nights	No. of light curves	No. of SPSS
BFOSC	Cassini	Loiano	2006 Aug–2015 Jul	33 (20)	119	85
DOLORES	TNG	La Palma	2007 May–2014 Aug	9 (5)	29	27
ALFOSC	NOT	La Palma	2014 Apr–2015 Mar	1 (1)	4	4
CAFOS	2.2 m	Calar Alto	2008 Sept–2012 May	7 (4)	21	17
EFOSC2	NTT	La Silla	2009 Apr–2015 Jan	3 (3)	19	17
LaRuca	1.5 m	San Pedro Mártir	2008 Jan–2011 May	33 (19)	113	86
ROSS	REM	La Silla	2007 Jul–2012 Jul	48 (27)	124	76
ROSS2	REM	La Silla	2015 Feb–2015 Jun	9 (7)	31	30
MEIA	TJO	Montsec	2009 Jun–2013 May	58 (24)	32	2

observed by *Gaia* as many times as possible. The mission requirement is to calibrate *Gaia* data with an accuracy of a few per cent (1–3 per cent) with respect to Vega (Bohlin 2007).

The obvious and fundamental requirement for a SPSS is that its magnitude (flux) is constant. Since only a few of our SPSS candidates have accurate enough photometry in the literature and have been monitored for variability in the past, it is very important to perform repeated and accurate observations of our targets in order to detect variability larger than 0.01 mag (if any), both intrinsic (e.g. pulsations) and extrinsic (i.e. binarity), before we invest a large amount of resources and observing time in getting their absolute SEDs. In addition, we remind that even stars used for years as spectrophotometric standards have been found to vary when dedicated studies have been performed (see e.g. G24−9, which has been found to be an eclipsing binary; Landolt & Uomoto 2007).

Additionally, a comprehensive search of the literature for each candidate analysed in this research was conducted. Most of our SPSS are white-dwarfs (WD) and hot subdwarfs, the remaining are dwarf/giant stars covering different spectral types from the hottest (O type) to the coolest (M type). WDs may show variability with (multiple) periods from about 1 to 20 min and amplitudes from about 1–2 per cent up to 30 per cent. We have tried to exclude stars within the instability strips for WDs of type ZZ Ceti, DQV, V777 Her or GW Vir (see Castanheira et al. 2007; Althaus et al. 2010, and references therein). However, in many cases the existing information is not sufficient (or sufficiently accurate) to firmly establish the constant nature of a given WD. Hence, many of our WD SPSS candidates needed to be monitored. Similar considerations are valid for hot subdwarfs (Kilkenny 2007).

Redder stars are also often variable: K stars have shown variability of 5–10 per cent with periods of the order of days to tens of days (Eyer & Grenon 1997); M stars can vary, for example, because of flares. In addition, binary systems are frequent and eclipsing binaries can be found at all spectral types. The periods of the known variables span from a few hours to hundreds of days, most of them having $P \sim 1$–10 d (Dvorak 2004).

The main use of the SPSS grid is of course the absolute calibration of *Gaia* spectrophotometric data. Nevertheless, such a large grid (more than 200 stars) represent an unprecedented catalogue of SPSSs, characterized by high precision and accuracy, full sky coverage, including stars spanning a wide range of spectral types, and with spectra covering a large wavelength range. For comparison, CALSPEC[2] (Bohlin 2007), containing the composite stellar spectra which are the fundamental flux standards for *Hubble Space Telescope* (*HST*) calibrations, consists of about 90 stars: our SPSS grid will be more than two times larger, and it will be about two times larger than the Stritzinger et al. (2005) catalogue. Our sample will be comparable to recent catalogues, such as the STIS Next Generation Spectral Library Version 2[3] which, in any case, does not meet as well all *Gaia* requirements (such as the magnitude range).

This paper is the third of a series (see Pancino et al. 2012; Altavilla et al. 2015, hereafter Paper I and Paper II, respectively), and presents the results of our short-term constancy monitoring campaign. It is organized as follows: the observation strategy and data reduction are briefly described in Section 2; Section 3 describes the light-curves production and our quality control (QC) procedures, and describes our criteria for constancy assessment; the results of the short-term constancy monitoring campaigns are presented and discussed in Section 4. We summarize our results and present our conclusions in Section 5.

2 OBSERVATIONS AND DATA REDUCTION

The various observing campaigns for the absolute flux calibration of the *Gaia* spectrophotometry (Paper I) are both spectroscopic and photometric. At survey completion, the SPSS observing campaigns amounted to 515 observing nights, at eight different telescopes and nine instruments (see Table 1), with 58 per cent useful data, and the rest lost due to bad weather, technical problems, or other reasons. The global campaign produced approximately 102 500 frames to be quality controlled, reduced, and analysed. The survey started in 2006 August and ended in 2015 July.

2.1 Photometry observations

Photometry observations were performed in two different flavours: *night points* or *time series*. The night point can be absolute or relative (depending on the sky conditions), and is formed by at least nine consecutive frames acquired in the Johnson–Cousins *B*, *V* and *R* filters (and sometimes also I and U). The study of SPSS absolute night points will be presented in a future dedicated paper (see Paper I for more details about the observing strategy details).

A time series contains at least 30 consecutive exposures in one filter (normally in the bluest available) covering approximately 1–2 h in order to monitor the short-term photometric constancy for each SPSS candidate. The actual duration of the 162 time series presented in this paper is illustrated in Fig. 1. We will focus here

[2] http://www.stsci.edu/hst/observatory/crds/calspec.html

[3] Sara R. Heap, NASA/Goddard Space Flight Center and Don Lindler, Sigma Space Corporation, http://archive.stsci.edu/prepds/stisngsl/

Downloaded from https://academic.oup.com/mnras/article/462/4/3616/2589704 by guest on 09 April 2021

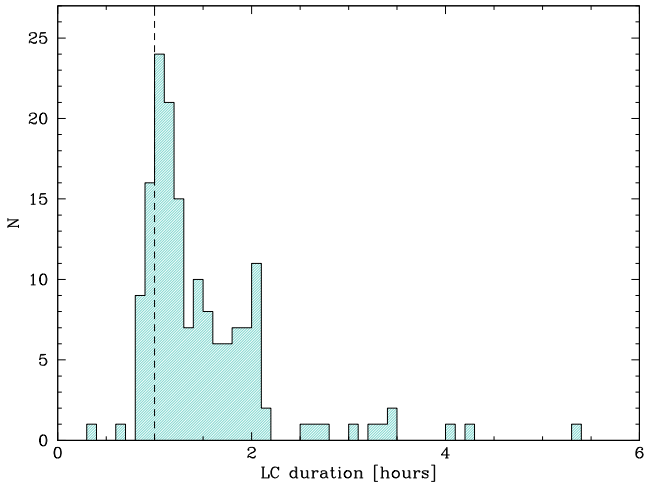

Figure 1. Distribution of time series durations for the 162 SPSS presented in this paper. A few series last less than 1 h (vertical dashed line), but the typical duration is 1.26 h with some curves lasting as long as 5.4 h.

on the analysis of time series in order to validate our SPSS candidates against short-term variability phenomena. Data coming from the night points obtained close to a time series were sometimes included, when useful and appropriate. We also use our preliminary results on the absolute night points to further investigate the long-term constancy of our SPSS candidates (see Section 4).

The candidate SPSS were prioritized according to available literature data, placing them more or less close to the main instability strips and variability regions across the parameter space. They were then observed, subject to the scheduling allocation of various observatories, and to visibility and weather constraints. The short-term constancy monitoring campaign shared the allocated time with the absolute photometry and the spectroscopy campaigns – approximately 143 nights were dedicated to it – and as a result was not always performed in optimal conditions. Consequently, not all candidate SPSS were observed, and some were observed with non-optimal data.[4] In addition to our study, *Gaia* observations themselves will further check variability, because each SPSS will be observed tens of times. Hidden, nearby companions may be discovered from space. These stars will simply be eliminated from the SPSS grid, which is built with some redundancy.

As can be seen from Table 1, each SPSS candidate was observed multiple times (on average, roughly three series per SPSS), either to repeat a non-optimal series, or to observe a subset of SPSS with different telescopes to compare the results. Here we present only the best time series obtained for each star.

2.2 Data reduction

To ensure that the maximum quality could be obtained from the SPSS photometric observations, a careful data reduction protocol (Marinoni et al. 2012) was implemented, following an initial assessment (Marinoni 2011; Marinoni et al. 2013) of all the instrumental effects that can have an impact on the photometry precision and accuracy. The methods and results of such instrumental effects study were presented in their final form in Paper II. Particularly relevant for the present paper are the characterizations of the *minimum acceptable exposure time*, the CCD linearity study, and the automated quality assessment and stability monitoring of the calibration frames (on time-scales as long as 9 years in some cases).

The data reduction methods were fairly standard but, due to the large amount of data collected, an automated IRAF-based[5] pipeline was built in order to take care of both the QC of the images and the removal of all the instrumental signatures. We applied the usual detrending steps including dark removal (for REM and MEIA), bias and overscan (when available) correction, flat fielding, bad pixel correction, and fringing correction when relevant.

2.3 Data availability

The raw and reduced data are stored at ASDC (ASI Science Data Center[6]) in a dedicated data base that will contain all the data products of the SPSS campaign and will be opened to the public with the first SPSS public data release in the near future. Additionally, the light curves presented in this paper will be published in the electronic version of the Journal and in the CDS Vizier service,[7] with the form illustrated in Table 2.

3 LIGHT CURVES

We describe here the procedure to obtain relative light curves from the aperture magnitude measurements on the single frames, the QC process, and the adopted criteria for constancy assessment.

3.1 Aperture photometry

Magnitudes were measured with SExtractor (Bertin & Arnouts 1996), a simple and powerful tool to perform reliable photometric measurements. We used the variety of flags and parameters output by the code to write the semi-automated procedures for the QC of our large data set.

Our observed fields are not crowded, and we aimed at very high precision (10 mmag or better), therefore we performed aperture photometry. We were free to choose an aperture large enough to avoid significant light losses; therefore we generally used six times the full width at half maximum (FWHM) that granted light losses well below 1 per cent.

The SExtractor catalogues were cross-matched with the catalogue cross-correlation software CataPack,[8] and in particular with the cataxcorr routine, to cross-identify the SPSS candidate and the comparison stars in each frame of a time series. A final catalogue was then created with the catacomb routine, containing the aperture magnitudes of the target SPSS and of suitable comparison

[4] Of the 212 initial candidates reported in Paper I, for 43 the kind of monitoring described in the present paper was not considered necessary because according to the available literature data the SPSS candidate was not close to any of the instability regions. Of the remaining list of 169 prioritized candidates for short-term monitoring, 162 could be observed with the described strategy and for seven we did not obtain usable data.

[5] IRAF is the Image Reduction and Analysis Facility, a general purpose software system for the reduction and analysis of astronomical data. IRAF is written and supported by the IRAF programming group at the National Optical Astronomy Observatories (NOAO) in Tucson, Arizona. NOAO is operated by the Association of Universities for Research in Astronomy (AURA), Inc. under cooperative agreement with the National Science Foundation.

[6] http://www.asdc.asi.it/

[7] http://vizier.u-strasbg.fr/

[8] The CataPack package is developed by P. Montegriffo at the Bologna Observatory (INAF). CataXcorr and CataComb are parts of this package, which are available at http://www.bo.astro.it/~paolo/Main/CataPack.html.

Downloaded from https://academic.oup.com/mnras/article/462/4/3616/2589704 by guest on 09 April 2021

Table 2. Best light curves for the 162 monitored SPSS. The columns contain: (1) the internal SPSS ID; (2) the SPSS name; (3) the instrument used; (4) the Heliocentric Julian day; (5) the photometric band; (6) the magnitude difference of each point with respect to the average magnitude of comparison stars; and (6) the errors of individual epoch measures for the SPSS (see text for more details). The relative photometry table is published in its entirety in the electronic online version of the Journal, and at CDS. Here we show just a few lines to illustrate its contents.

SPSS	Star name	Instrument	HJD (d)	Band	Δm (mag)	δ_m (mag)
042	P 41-C	BFOSC	2454877.67853892	*B*	−0.0000	0.0013
042	P 41-C	BFOSC	2454877.68073774	*B*	0.0010	0.0015
042	P 41-C	BFOSC	2454877.68225397	*B*	0.0025	0.0014
042	P 41-C	BFOSC	2454877.68536727	*B*	−0.0013	0.0016
042	P 41-C	BFOSC	2454877.68676764	*B*	0.0017	0.0015

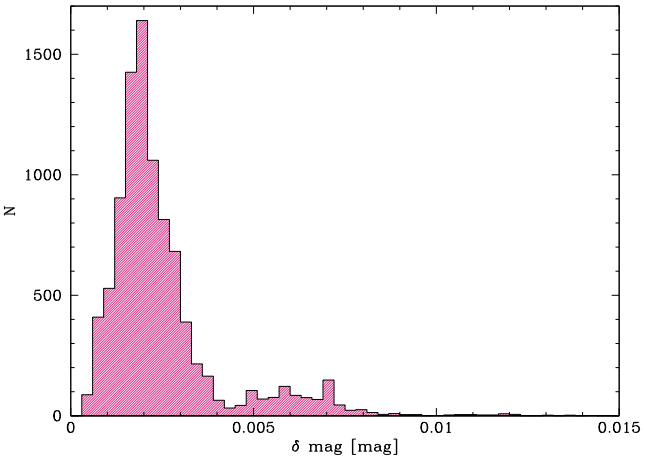

Figure 2. Histogram of the errors on the differential SPSS magnitudes for each epoch, based on SExtractor formal errors on the aperture magnitudes. The histogram contains 9377 single-epoch catalogues used to build the best light curves presented in this paper.

stars in the field, which should be visible in all the frames included in a series. We selected at least two bright stars around the SPSS, and monitored the magnitude difference between the target and the comparison stars, as described in more detail in Section 3.3. If one of the comparison stars was found to be variable, it was rejected from the adopted set of comparison stars.

The errors on the differential SPSS magnitudes (δmag) – based on the formal SExtractor errors on the aperture magnitudes for each epoch – are displayed in Fig. 2. The histogram contains 9377 single-epoch catalogues, used to build the best light curves presented in this paper. As can be seen, the typical error is 0.002 mag, with some measurements reaching as high as 0.01 mag and more, but also many going as low as 0.0005 mag.

Instrumental effects were investigated in detail in Paper II, as mentioned previously, and taken into account as explained there. Briefly, we decided to exclude from the present analysis all the images affected by low signal-to-noise ratio (S/N), saturation, non-uniform CCD illumination or significant geometric distortions. A few dubious cases in which atmospheric conditions were not optimal are discussed in Section 4. Moreover, the use of strictly differential photometry ensures that all remaining systematic or instrumental error sources are kept below the 1 per cent level – which is our requirement for *Gaia* – and therefore were not explicitly considered in the error computation.

3.2 Quality control

Because we required a high precision in the final light curves, great care was taken in the selection of appropriate frames and time series for the analysis, with three levels of automated QC. At the *star level*, both the SPSS and the candidate comparison stars measurements had to satisfy a set of criteria: S/N > 100, no saturation (using the measurements presented in Paper II), non-distorted point spread function, seeing below 5 arcsec, and no bad pixels within the selected aperture. At the *frame level*, we rejected frames in which the SPSS did not pass the star level QC, or where there were less than two comparison stars passing the star level QC. Finally, at the *series level*, we only accepted time series with at least 30 exposures passing the frame level QC, and lasting in total at least one hour.

The QC procedure issues warnings that can be examined later to assess the causes. In fact, our QC criteria are quite restrictive, and in some cases we were forced to accept some series that did not actually pass all of the QC chain. For example, when no better series existed for a particular SPSS, we accepted series slightly shorter than 30 points, or with one comparison star only, or with a large spread in the average comparison star magnitudes. We used these less precise data anyway to put some constraints on the maximum variation amplitude allowed by the data on the tested time-span of 1–3 h, as further discussed in Sections 3.4 and 4.

The actual duration of the 162 time series presented in this paper is illustrated in Fig. 1. It can be seen that a few light curves shorter than 1 h were included for lack of better data, while the typical duration is 1.26 h, with a few curves lasting 4 h or more.

3.3 Light-curves production

Using the catalogues that passed the QC criteria already described in Section 3.2, we built the light curves in two main steps. In the first step we created a *super-comparison* light curve using all the chosen comparison stars. At each epoch, the average flux of the chosen comparison stars was computed and converted into an average epoch magnitude. For each star, the difference between its epoch magnitude and the average epoch magnitude above was then used to build a light curve. The light-curve of comparison stars were reported to the same zeropoint using the difference between the median magnitude of each curve with that of a chosen comparison curve, usually the one of the star with the highest S/N (see bottom panel of Fig. 3). The super-comparison curve (magenta line in Fig. 3) was then created as the average of normalized light curves for all the chosen comparison stars.

As a second step, the SPSS light curve was computed and normalized to zero. This was achieved by first computing the SPSS

Downloaded from https://academic.oup.com/mnras/article/462/4/3616/2589704 by guest on 09 April 2021

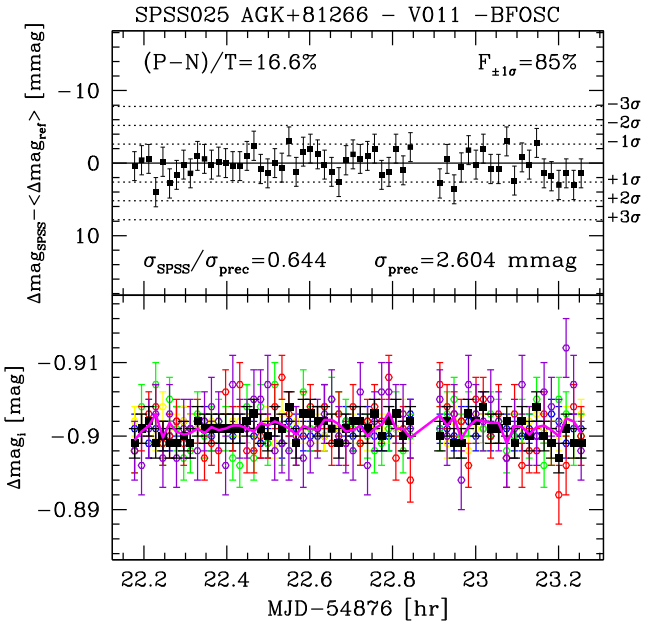

Figure 3. An example of checkplot produced by our light-curve pipeline. The star is AGK+81266, our SPSS 025, observed from Loiano with BFOSC@Cassini, in our run V-011 (2009 February). In the bottom panel are the normalized light curves of the SPSS (in black) and of a few comparison stars (each in a different colour), as a function of the Modified Julian Day (MJD). The super-comparison light curve is also plotted as a magenta curve. In the top panel the zeroed light curve for the SPSS is plotted, along with some useful quantities for light-curve validation and SPSS constancy assessment (see text for more details). The dotted lines mark the ±1, 2, and 3 $\sigma_{\rm prec}$ thresholds.

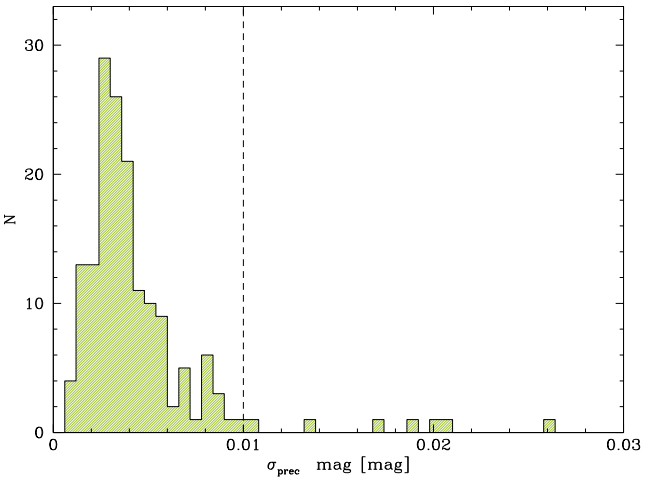

Figure 4. Histogram of $\sigma_{\rm prec}$ of the 162 light curves presented in this paper. The vertical dashed line marks our criterion of 0.01 mag. As can be seen, the typical curve precision is of 0.004 mag and there are only seven light curves that do not match our criterion, and that were included for lack of better data.

normalized light curve in the same way as for the comparison stars (black filled circles in the bottom panel of Fig. 3) and then by subtracting the super-comparison curve from it (top panel of Fig. 3).

A number of useful quantities were also computed along with a checkplot that summarizes all relevant information (Fig. 3). The quantities that were used for the light-curve QC and constancy assessment are the following:

(i) $\sigma_{\rm prec}$ is the average standard deviation of the reference stars and tracks the precision to which the magnitude of constant stars is reproduced over the whole series;

(ii) $\sigma_{\rm SPSS}$ is the standard deviation of the SPSS light curve;

(iii) the ratio $\sigma_{\rm SPSS}/\sigma_{\rm prec}$ is an indication of variability: when this ratio is above one, the variation detected in the SPSS light curve is larger than the curve precision; there is a significant indication of variability when the ratio becomes higher than 3;

(iv) $F_{\pm 1\sigma}$ is the fraction of SPSS light-curve points lying within $\pm 1\sigma_{\rm prec}$; similarly to the ratio described above, this is another way of searching for variability: when the fraction is significantly below 68 per cent, the distribution of points is not normal;

(v) finally, $(P - N)/T$ is a fractional indicator of asymmetry in the distribution of points, where P is the number of points above zero, N below zero, and T the total number of points in the curve.

After light-curve production, a simple QC criterion is applied: $\sigma_{\rm prec} \leq 10$ mmag. Ideally, constancy assessment is relevant for *Gaia* only when based on light curves passing this criterion. In practice, as mentioned previously, for some SPSS we also accepted curves that did not pass the criterion, for lack of better data, because we assumed that even some less strict indication of the SPSS nature was better than no indication at all. The distribution of $\sigma_{\rm prec}$ for the 162 light curves presented in this paper is shown in Fig. 4, where it can be noticed that seven light curves failing this QC step were included. We note that the typical precision of our light curves is comparable to that of recent studies for the search of exoplanets from space (Nascimbeni et al. 2012) or from the ground (Klagyivik et al. 2016).

An output file containing the resulting (relative) light curve for each time series of each SPSS was produced and archived at ASDC. The best light curve for each SPSS, presented in this paper, is also published electronically in the form presented in Table 2.

3.4 Constancy assessment

The simplest form of variable star analysis is the inspection of the shape of the light curve, and the time and magnitude of maximum and minimum, if any. The term *range* is here adopted to denote the difference between maximum and minimum (if present), or the maximum magnitude excursion observed in the curve if no clear maximum and minimum are detected. The term *amplitude* (A) is used to denote the half range, as in the coefficient of a sine or cosine function.

For the light curves passing our QC criterion ($\sigma_{\rm prec} \leq 10$ mmag), we contemplate two cases:

(i) a candidate SPSS is validated as *constant* over the sampled periods if no coherent pattern is present in the light curve and if $\sigma_{\rm SPSS}/\sigma_{\rm prec} \lesssim 1.5$ (see Fig. 5);[9] in that case, even if the star varies, its amplitude is $A < \sigma_{\rm SPSS} \pm \sigma_{\rm prec}$ and it is accepted as an SPSS;

(ii) a candidate SPSS is judged *variable* and rejected as an SPSS if a coherent pattern is evident; in this case, we define $A_{\rm max} = \max(LC_{\rm max}, |LC_{\rm min}|)$, where $LC_{\rm max}$ and $LC_{\rm min}$ are the maximum and minimum magnitude differences measured on the LC, and if

[9] This is not a strict limit, but all stars close to this value were checked more carefully than the ones far away from it. A posteriori, we can say that the median value of $\sigma_{\rm SPSS}/\sigma_{\rm prec}$ is 0.91 for the constant stars, 1.05 for the likely constant stars, 1.97 for the suspect variables, and 5.64 for the confirmed variables, as shown in the Fig. 5.

Downloaded from https://academic.oup.com/mnras/article/462/4/3616/2589704 by guest on 09 April 2021

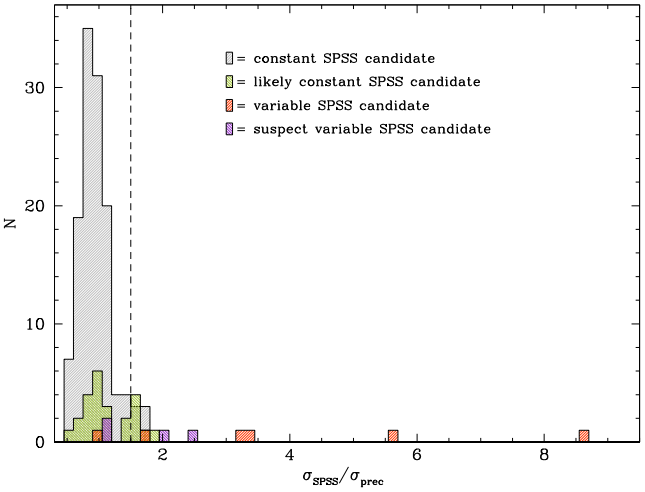

Figure 5. Histogram of $\sigma_{SPSS}/\sigma_{prec}$ of the 162 light curves presented in this paper. The vertical dashed line marks our approximate limit for constancy. The constant stars are highlighted in grey, the likely constant ones in green, the suspect variable stars in purple, and the confirmed variable stars in orange.

$A_{max} > 3\sigma_{prec}$ the pattern is significant; the estimated amplitude of the variation is:

(a) if no clear maximum or minimum is visible in the curve, the period of the variation is most probably longer than the time series, and we assumed that $A > A_{max} \pm \sigma_{prec}$;
(b) if only the maximum or minimum is visible in the curve, the period of the variation is again most probably longer than the time series, but we assumed that $A \geq A_{max} \pm \sigma_{prec}$;
(c) if both the maximum and minimum are visible, we assumed $A = A_{max} \pm \sigma_{prec}$, but of course this is only valid over the sampled periods.

As can be seen, the criteria can lead to dubious cases, for which additional checks have to be performed and a discussion of special cases can be found in Section 4. For the curves that do not pass the QC because $\sigma_{prec} > 10$ mmag or because they failed any other of the QC levels described previously, we still attempted a constancy assessment, although with less stringent results:

(i) if no clear pattern was present in the light curve, and if the various indicators described in the previous section were compatible with a normal distribution, we validated the SPSS candidate as *likely constant* and kept it in the SPSS sample; in this case, we set the allowed amplitude of the variation, if present, as $A < 3\sigma_{SPSS} \pm \sigma_{prec}$;
(ii) if some coherent pattern was present, the star was judged *suspect variable*; in that case the amplitude was assigned with the same criteria used for variable stars and the candidate SPSS was removed from the candidate SPSS list.

3.5 Additional criteria

We originally planned and started an additional constancy monitoring campaign on longer time-scales (see Paper I) with the goal of observing each SPSS candidate four times per year for 3 years. However, because we mostly obtained the observing time each semester at six different facilities with normal time applications,[10] it was not practically possible to obtain regularly the required sampling. We therefore stopped our long-term campaign also because it became apparent that *Gaia* itself will be able to perform this kind of monitoring excellently on the SPSS sample.

We instead used the absolute night points (see Section 2) of our absolute photometry campaign that are presently being analysed (Galleti et al., in preparation). We have at least three independent night points per SPSS candidate, and in some cases they cover up to 6 years or more for a single SPSS. Therefore, in some difficult cases we could use absolute night points to investigate suspicious trends found in our short-term light curves or claims of long-term variability found in the literature. Some examples of this kind of additional checks can be found in the discussions in the next section. Additionally, a thorough literature search for each of the candidate SPSS presented here was carried out.

4 RESULTS

We were able to perform the constancy assessment on a total of 162 SPSS candidates. As a result, 150 SPSS candidates were validated against short-term variability, and only 12 were rejected (eight being clearly identified as variable stars, and four being classified as suspect variable stars).

We needed to either reject or retain each SPSS, therefore for some uncertain cases we had to take decisions, motivated by more than the simple criteria described in the previous section. We discuss in the following the most difficult cases, both to illustrate the assessment procedure, and to provide useful information for future studies of these stars. The best light curves obtained for each SPSS are displayed in Fig. 6, and the outcome of the assessment procedure is summarized in Table 3, along with some other useful information.

4.1 Control cases

The first three SPSS candidates are the *Pillars*, three pure hydrogen WDs adopted by Bohlin, Colina & Finley (1995) as fundamental calibrators (see also Paper I). We expect these extremely well studied stars to be constant, and therefore we observed them as control cases to verify that with our criteria they turned out as constant stars. Indeed, even for GD 153 (SPSS 003) that was observed in a windy night with high and variable seeing and some veils, we found $\sigma_{prec} = 0.005$ mag and no sign of variability. We conclude that even in the presence of veils our method can be applied.

4.2 Constant stars

Of the 126 candidate SPSS that successfully passed all the QC criteria and were judged constant, five deserve to be discussed.

A slight trend was observed for GRW+705824 (SPSS 015), especially towards the end of the light curve (see Fig. 6). Even if the trend was within ±5 mmag, this could be an indication of longer term variability. We note that veils appeared during the light curve, and the seeing got worse towards the end of the series. In spite of all these effects, the curve is of very high quality ($\sigma_{prec} = 0.0017$ mag). Only recently, Bohlin & Landolt (2015) found some weak indication of a 0.004 mag yr^{-1} variability after monitoring it from 1986 to

[10] With the exceptions of: NTT, for which we obtained once the ESO large programme status; Calar Alto, for which we obtained a few years of granted time; and TNG, for which we obtained a medium-sized programme allocation once.

Downloaded from https://academic.oup.com/mnras/article/462/4/3616/2589704 by guest on 09 April 2021

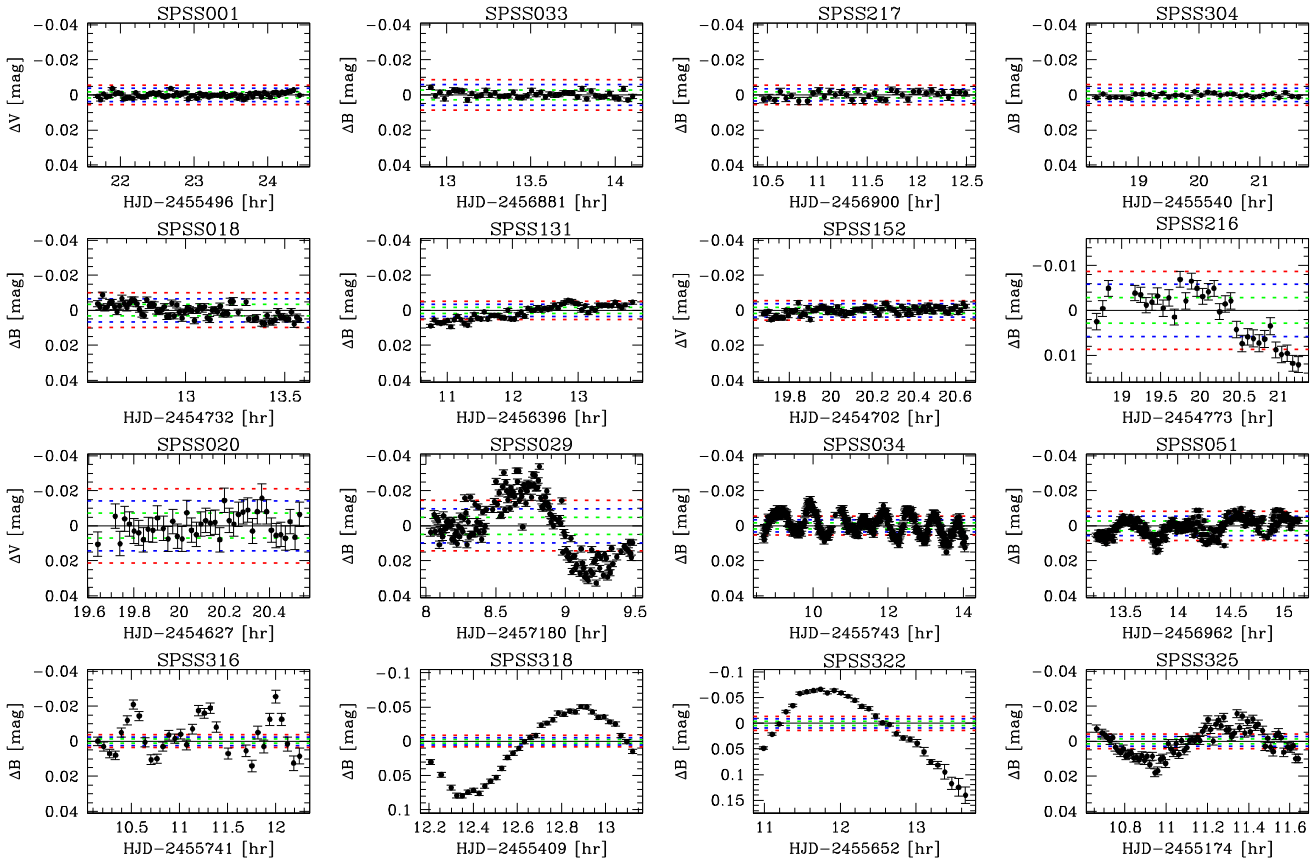

Figure 6. The best light curve for each monitored SPSS candidate is displayed in each panel using the same magnitude scale, when possible. The figure is available in its entirety in the electronic version of the Journal. Here we show some example of constant stars (the first four panels), suspect variable stars (panels five to eight; these stars are discussed in Section 4.4), and confirmed variable stars (the remaining panels, these stars are discussed in Section 4.5). This is the final zeroed light curve as in the top panel of Fig. 3. The differential magnitudes are in the sense SPSS minus supercomparison (see text for more details), i.e. negative values mean that the SPSS becomes brighter. The ±1, 2, and 3 $\sigma_{\rm prec}$ thresholds are marked by coloured dotted lines in each panel.

1991. We thus checked our absolute night points spanning 3 years (from 2009 to 2012), and found no significant variation within 0.0065 mag.

Similarly, the well-studied Feige 110 (SPSS 023) shows a weak trend along the time series, still contained within ±5 mmag, possibly because the sky was veiled during the curve acquisition. In the literature, no previous detection of variability was found. Our absolute night points show large variations in the *B* and *R* bands over one year, but there appear to be problems in the data quality and analysis for this particular set. On the other hand, the corresponding *V* magnitude appears constant within 0.007 mag. Therefore, we accept this SPSS candidate.

Another similar case is 1812095 (SPSS 037), with a weak trend contained in the ±5 mmag range, clear sky observations, and no sign of variability in the literature. Our absolute photometry data contain only one reliable night point, so we cannot use it as an additional constraint.

A different problem was apparent for WD 2028+390 (SPSS 203), where the only available curve was probably interrupted for the nitrogen refilling of the instrument and therefore a small jump appears between the two branches of the light curve. Nevertheless, the SPSS candidate appears constant within 4 mmag and the curve is of good quality.

Finally, SDSS J125716+220059 (SPSS 355) shows a trend, entirely contained within ±10 mmag, that is most probably caused by the high (from ≃5 to 7 arcsec) and variable seeing, with thin clouds, during observations. No other curves were obtained for SPSS 355. No sign of variability was found in the literature, and our absolute photometric measurements are always contained within a few mmag. So we decided to retain this SPSS candidate.

4.3 Likely constant stars

We retained as likely constant 24 SPSS candidates that formally failed some QC level, or did not completely fulfil our constancy criteria.

One example of likely constant stars are SPSS candidates for which only one of the field comparison stars passed all QC steps, generally because the other comparison stars were too faint (S/N below 100). In most cases, including one or more faint reference stars did not significantly improve the quality of the curve, while in a few cases, including a second comparison stars with S/N below 100 provided better results. Examples of these SPSS are: EG 21 (SPSS 005), LTT 9491 (SPSS 022), SA 107−544 (SPSS 032), LTT 1020 (SPSS 039), WD 1105−048 (SPSS 121), WD 1211−169 (SPSS 129), G 16−20 (SPSS 134), WD 0501−289 (SPSS 170),G 179−54 (SPSS 192), WD 0123−262 (SPSS 220), and GJ 507.1 (SPSS 335).[11] For all these stars we did not detect any clear sign of variability and no variability indication was found in the literature or in our absolute photometry night points. Of these, SPSS 121

[11] For SPSS 335 all the available comparison stars failed all QC steps.

Downloaded from https://academic.oup.com/mnras/article/462/4/3616/2589704 by guest on 09 April 2021

Table 3. Results. The columns contain: (1) the SPSS internal ID; (2) the name of the star; (3) and (4) the star coordinates compiled in Paper I; (5) the spectral type compiled in Paper I; (6) the instrument used; (7) photometric band of the best observed time series; (8) the sky quality during the acquisition of our best time series; (9) indicates whether the following column is an upper ($\leq$) or lower ($\geq$) limit or a determination ($=$) of the amplitude; (10) the minimum tested amplitude in case of constant stars, or the maximum observed amplitude in case of variable stars; (11) the precision of the light curve used (see text); (12) the number of comparison stars used for the SPSS light-curve production; (13) specifies whether the star will be used as a *Gaia* SPSS; (14) any additional comment. The table is available in its entirety in the electronic version of the Journal and at CDS. Here we show a portion to illustrate its contents.

SPSS	Name	RA (J2000) (hh:mm:ss)	Dec. (J2000) (dd:mm:ss)	Sp Type	Instrument	Band	Sky quality	Lim	A (mag)	$\sigma_{\rm prec}$ (mag)	No. of comp. stars	Verdict	Notes
001	G 191-B2B	05:05:30.61	+52:49:51.95	DA0	LaRuca	*V*	Good	$\leq$	0.0014	0.0019	3	Accepted	Pillar, control case
002	GD 71	05:52:27.63	+15:53:13.37	DA1	LaRuca	*B*	Good	$\leq$	0.0026	0.0034	3	Accepted	Pillar, control case
003	GD 153	12:57:02.33	+22:01:52.52	DA1	BFOSC	*B*	Windy	$\leq$	0.0049	0.0050	2	Accepted	Pillar, control case. Bad seeing
005	EG 21	03:10:31.02	−68:36:03.39	DA3	EFOSC2	*B*	Veiled	$\leq$	0.0056	0.0011	1	Accepted	Likely constant. Only one comparison
008	LTT 3218	08:41:32.56	−32:56:34.90	DA	EFOSC2	*B*	Good	$\leq$	0.0032	0.0038	2	Accepted	–
009	LTT 2415	05:56:24.74	−27:51:32.35	G	ALFOSC	*B*	Good	$\leq$	0.0042	0.0036	2	Accepted	–
010	GD 108	10:00:47.37	-00: 33:30.50	B	LaRuca	*B*	Veiled	$\leq$	0.0065	0.0082	3	Accepted	–
011	Feige 34	10:39:36.74	+43:06:09.25	DO	BFOSC	*B*	Veiled	$\leq$	0.0032	0.0037	3	Accepted	–
012	LTT 4364	11:45:42.92	−64:50:29.46	DQ6	ROSS2	*g*	Good	$\leq$	0.0032	0.0037	4	Accepted	–
013	Feige 66	12:37:23.52	+25:03:59.87	O	LaRuca	*B*	Veiled	$\leq$	0.0063	0.0079	2	Accepted	–
014	HZ 44	13:23:35.26	+36:07:59.51	O	DOLORES	*B*	Cloudy	$\leq$	0.0031	0.0055	2	Accepted	–
015	GRW+705824	13:38:50.47	+70:17:07.62	DA3	BFOSC	*B*	Veiled	$\leq$	0.0018	0.0017	2	Accepted	Possible trend, but A <5mmag
017	LTT 7987	20:10:56.85	−30:13:06.64	DA4	EFOSC2	*B*	Good	$\leq$	0.0028	0.0027	2	Accepted	–
018	BD+284211	21:51:11.02	+28:51:50:36	Op	BFOSC	*B*	Good	$\geq$	0.0088	0.0033	3	Rejected	Suspect variable
020	BD+174708	22:11:31.37	+18:05:34.17	F8	ROSS	*V*	Varying	$\leq$	0.0065	0.0071	2	Rejected	Long term variability
021	LTT 9239	22:52:41.03	−20:35:32.89	F	ALFOSC	*B*	Good	$\leq$	0.0152	0.0030	2	Accepted	Likely constant, possible trend
022	LTT 9491	23:19:35.44	−17:05:28.40	DB3	EFOSC2	*B*	Veiled	$\leq$	0.0159	0.0039	1	Accepted	Likely constant. Only one comparison
023	Feige 110	23:19:58.40	−05:09:56.21	O	BFOSC	*B*	Veiled	$\leq$	0.0026	0.0029	5	Accepted	Possible trend, but A <5mmag
024	HILT 600	06:45:13.37	+02:08:14.70	B1	LaRuca	*B*	Good	$\leq$	0.0034	0.0040	3	Accepted	–
025	AGK+81266	09:21:19.18	+81:43:27.64	O	BFOSC	*B*	Good	$\leq$	0.0017	0.0026	5	Accepted	–
026	Feige 56	12:06:47.23	+11:40:12.64	B5p	BFOSC	*B*	Veiled	$\leq$	0.0332	0.0108	2	Accepted	Likely constant. Less than 1 h
027	Feige 67	12:41:51.79	+17:31:19.75	O	BFOSC	*B*	Veiled	$\leq$	0.0031	0.0030	5	Accepted	–
028	SA 105−663	13:37:30.34	−00:13:17.37	F	BFOSC	*B*	Veiled	$\leq$	0.0068	0.0079	2	Accepted	–
029	SA 105–448	13:37:47.07	−00:37:33.02	A3	BFOSC	*B*	Good	$=$	0.0338	0.0048	2	Rejected	Variable

Downloaded from https://academic.oup.com/mnras/article/462/4/3616/2589704 by guest on 09 April 2021

was found to be a magnetic star (Aznar Cuadrado et al. 2004) in a wide binary system (Koester et al. 2009; Zuckerman 2014), SPSS 129 is not a WD being a G8IV star (Kharchenko & Roeser 2009), and SPSS 134 is suspected to be a member of a wide binary system (Zapatero Osorio & Martín 2004). These findings do not pose significant danger to the use of these candidate SPSS, so they were retained in the *Gaia* SPSS grid.

Another example concerns time series having too few points (less than 30) or lasting less than one hour, like: Feige 56 (SPSS 026), HD 121968 (SPSS 030), G 184−20 (SPSS 140), WD 1918+725 (SPSS 142), WD 1319+466 (SPSS 246), WD 1637+335 (SPSS 254), WD 1034+001 (SPSS 308), SDSS J233024.89–000935.1 (SPSS 321), and LP 885−23 (SPSS 352). Each star suffered from various other drawbacks like low S/N in the SPSS as well, or veils and other weather problems. In any case, the remaining points generally showed no clear sign of variability and no variability was found in the literature or in our absolute photometry. Zapatero Osorio & Martín (2004) noted that SPSS 140 is part of a wide binary system. SPSS 254 was also reported as non-variable by McGraw (1977), Dolez, Vauclair & Koester (1991), and Gianninas, Bergeron & Fontaine (2005).

One star, WD 2216−657 (SPSS 276), did not pass the criteria because the S/N of the SPSS was lower than 100 in the only curve available. However, the curve precision was acceptable ($\sigma_{\rm prec}$ = 0.008 mag) and no sign of coherent trends or variability was detected. Our absolute photometry is stable within 0.015 mag and no indication of variability was found in the literature either.

Finally, three stars showed coherent patterns in their light curves, although they roughly remained within the actual variability limit of 0.01 mag. The first one, LTT 9239 (SPSS 021), a widely used flux standard, was observed in good conditions and our absolute photometry did not show any significant variation. The second, WD 0943+441 (SPSS 180), was considered non-variable by Kepler et al. (1995) who found it constant within 0.0051 mag. The third WD 0954−710 (SPSS 181) was observed with ROSS2 when there was a problem with the dichroic, no sign of variability was found in the literature, and our absolute photometry was all contained within 0.004 mag over 6 years.

4.4 Suspect variable stars

Similarly to the likely constant case, some candidate SPSS were classified as suspect variable stars either because the data did not formally pass the QC but some significant trends were revealed, or because we identified significant trends, but without finding a definite maximum or minimum in the light curve. Four candidate SPSS were judged suspect variables and removed from the SPSS candidate list.

The first one is BD+284211 (SPSS 018), a star present in the Landolt & Uomoto (2007) catalogue and a widely used CALSPEC standard (Bohlin 2007). The trend we observe has an amplitude of almost 0.010 mag in the *B* band, and although this trend is still formally within $3\sigma_{\rm prec}$, we clearly do not sample the entire period: the variation is therefore likely to exceed our criteria. In addition, there are hints in the literature that this star might be peculiar in many respects. It has a 5 mag fainter red companion at about 3 arcsec (Massey & Gronwall 1990) as shown also by our data in Fig. 7, and it has emission in both Hα and some metallic emission lines in the optical band (Herbig 1999; Latour et al. 2013). It is a suspect binary based on its measured infrared excess (Ulla & Thejll 1998) and has X-ray emission (La Palombara et al. 2014; Latour et al. 2015).

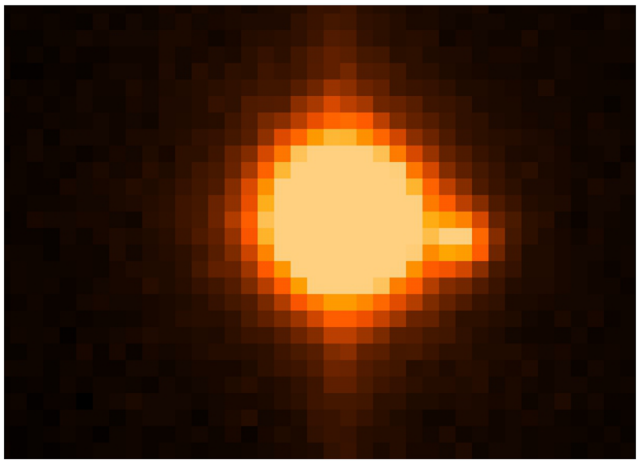

Figure 7. One of the *V*-band images of BD+284211 (SPSS 018) obtained at Calar Alto with CAFOS showing the presence of a red companion at a distance of about 3 arcsec.

The second one is WD 1327−083 (SPSS 131). This star was classified as non-variable by Giovannini et al. (1998). Nevertheless, we observe a clear variation of about 0.015 mag in a high-quality curve lasting more than 3 h and our absolute photometry data show a variation of 0.04 mag in *B* band in slightly less than one year. The period observed in the light curve is too long to be compatible with the typical periods of pulsations for ZZ Ceti stars: perhaps SPSS 131 could be a multiple object.

The spectroscopic binary G 190−15 (SPSS 152) was classified as single-lined spectroscopic binary by Latham et al. (2002) and later as double-lined specrtoscopic binary by Halbwachs et al. (2014). The level of optical variability was uncertain in the past. Our best light curve shows a possible trend that is contained within ±5 mmag and could thus in principle be ignored as done for a few stars in the previous sections. The curve quality was quite good. However, our absolute photometry, spanning 3 months, showed a variation of 0.03 mag in *B*, that is above our limit of 0.01 mag.

The last star, WD 0009+501 (SPSS 216), is a magnetic WD, the first one discovered below 100 kGauss (McCook & Sion 1999). While we could find no study reporting light curves or variability detections, we observe a variation of about 0.013 mag in a high-quality light curve, lasting approximately 2.5 h. The first part of the light curve is quite flat and then the curve declines, so we could not detect any clear maximum or minimum. No apparent technical problems could explain the trend, but we prefer to avoid using this star in the *Gaia* SPSS grid.

4.5 Confirmed variable stars

Eight of the SPSS candidates in our original list (reported in Paper I) are now known to be variable and were rejected from the candidate SPSS list.

The first one is BD+174708 (SPSS 020), a well-known and widely used CALSPEC standard that was also selected as target by the ACCESS rocket mission (Kaiser et al. 2014). It was shown to brighten by 0.04 mag over a period of 5 years by Bohlin & Landolt (2015). Our absolute photometry data also show a variation of 0.03 mag in the *B*, *V*, and *R* filters over a period of 7 years. Even if our short-term data do not show any variation in the monitoring period of 1 h, we clearly cannot use it as a *Gaia* SPSS.

Downloaded from https://academic.oup.com/mnras/article/462/4/3616/2589704 by guest on 09 April 2021

SA 105−448 (SPSS 029) is another widely used photometric standard stars in the Landolt (1983) catalogue (see also Stritzinger et al. 2005). Our best light curve shows a very definite variability pattern with an amplitude of 0.034 ± 0.005 mag in *B* band, compatible with δ Scuti type pulsations. We do see in the LC one minimum and one maximum separated by roughly 0.5 h. Among the numerous studies employing this star as a standard, we could find no indication of variability. Unfortunately, we have only one absolute night point of non-optimal quality. We found data for this star in NSVS (Northern Sky Variability Survey; Woźniak et al. 2004). A preliminary analysis of the NSVS data shows a variation with a period of roughly one hour and amplitude ≃0.03 mag in the *V* band.

Another star that was already shown to be variable (see also Paper I) is 1740346 (SPSS 034). We publish here a longer light curve with respect to that paper (6 h), showing various maxima and minima. Its maximum amplitude is 0.015 ± 0.002 mag in the *B* band, with various periods and amplitudes. It was proposed to be a δ Scuti star by Marinoni (2011).

Unluckily, another candidate SPSS that was selected to be in common with the targets of the ACCESS mission also turned out to be variable: HD 37725 (SPSS 051). Its light curve shows an unmistakable variation over a time-scale of roughly half an hour or less, and a maximum amplitude of 0.015 ± 0.003 mag in *B* band. Our light curve covers almost two hours and a clear global brightening in the variation pattern is visible. The star is an A3 V and there is evidence of multiple periods, therefore it is likely a δ Scuti star.

Among the several SPSS selected from the SEGUE (The Sloan Extension for Galactic Understanding and Evolution; Beers et al. 2004; Yanny et al. 2009) sample to fill in a few under-represented spectral types, four showed clear signs of variability, with amplitudes ranging from 0.018 ± 0.001 to 0.079 ± 0.003 mag. The first one, SDSS J164024.18+240214.9 (SPSS 316), was classified as a candidate blue horizontal branch star by Xue et al. (2008), but not confirmed by spectroscopy. Due to the evidence of multiple periods in the light curve, it could be a variable of the δ Scuti type. For this star, we found some data in NSVS, CSS (Drake et al. 2009, Catalina Sky Survey), and Wide-field Infrared Survey Explorer (*WISE*) (Cutri et al. 2013). However the data have not sufficient quality to draw any firm conclusion.

The second one, SDSS J224204.16+132028.6 (SPSS 318), was classified as a blue straggler by Xue et al. (2008). Again its light curve is compatible with a δ Scuti family pulsator with a clear minimum and maximum separated by ≃40 min. From a preliminary analysis of data available in CSS, we confirm a variation with an amplitude of roughly 0.05 mag and a period of ≃50 min.

The third one, SDSS J122241.66+422443.6 (SPSS 322), has been recently included in the list of RR Lyrae discovered in the SDSS-Pan-STARRS-Catalina footprint (Abbas et al. 2014).

The last one, SDSS J000752.22+143024.7 (SPSS 325), has no specific mention of variability in the literature, but it has low amplitude pulsation and a period compatible with those of a δ Scuti star.

Finally, we note that – even if we did not obtain any useful data – SDSS J204738.19−063213.1 (SPSS 317) was reported to be an RR Lyrae star by Abbas et al. (2014). Therefore, this SPSS was excluded from our candidate list.

4.6 Variable comparison stars

Among the field stars that could be used as comparison, we found three that were variable.

The first one was initially chosen as comparison star for the light curve of WD 1659–531 (SPSS 196), as shown in the first panel of Fig. 8, and later rejected because of its clear variability pattern. Its light curve is shown in the upper panel of Fig. 9. It was identified as 2MASS J17025022−5315592, but no further information was found in the literature. In our light curve, lasting 1.2 h, we could not observe any clear maximum or minimum but the range of the variation is at least 0.1 mag in *B* band.

The second one was a comparison star for WD 0123–262 (SPSS 220), with its position and light curve reported in Figs 8 and 9, respectively. The star was identified as 2MASS J01252029−2602141, but also in this case no further information was found in the literature. We observe a variation of about 0.1 mag in *B* band, with a possible double minimum towards the end of the curve. The CSS data show a typical RR-Lyrae light curve with an amplitude of ≃0.5 mag and a period of ≃0.57 d. The double minimum we observed in our data is caused by the typical luminosity bump associated with the early shock phase in RRab variables.

The last one was one of the comparison stars for the light curve of WD 0859–039 (SPSS 307), as shown in Figs 8 and 9. It was identified as 2MASS J09015726−0411010, an eclipsing binary of W Ursae Majoris type, with a period of 0.420 775 d by the NSVS. In our curve we observed a variation of about 0.25 mag in *B* band.

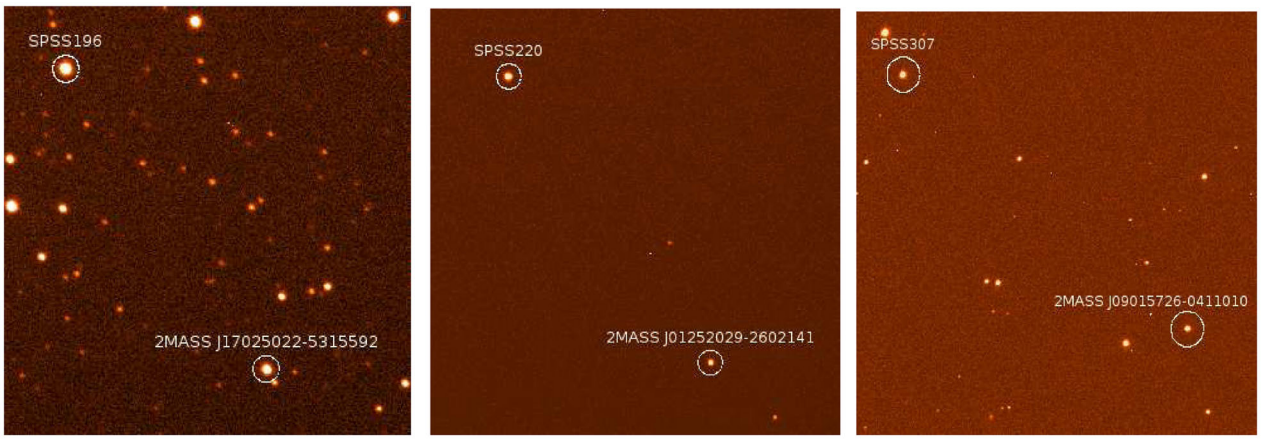

Figure 8. Finding charts of the three comparison stars found variable during our survey. In all charts, north is up and east is left. The field of view is ≃ 2, 2, and 7 min from left to right, respectively.

Downloaded from https://academic.oup.com/mnras/article/462/4/3616/2589704 by guest on 09 April 2021

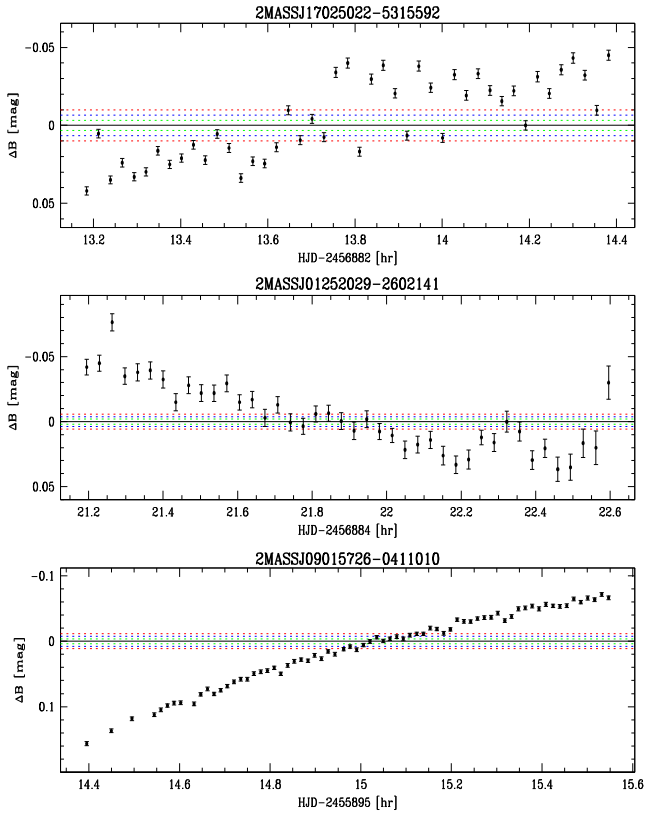

Figure 9. Light curves of the three comparison stars found variable during our survey.

5 CONCLUSIONS

We presented the results of our extensive short-term (1–2 h; see also Fig. 1) constancy monitoring campaign of 162 candidate SPSS from the list reported in Paper I, which needed this kind of monitoring. A total of approximately 143 observing nights – on a grand-total of more than 515 dedicated to the *Gaia* SPSS grid ground-based campaigns – were dedicated to the short-term constancy monitoring. We present in this paper the best available curve for each of the monitored SPSS candidates, but on average we obtained approximately three curves for each candidate SPSS. The typical precision of the light curves was 4 mmag (see also Fig. 4).

We presented and discussed the criteria adopted to assess the constancy or variability of the candidate SPSS. When the candidate SPSS were judged constant or likely constant, because no clear variability pattern was present and the maximum amplitude allowed by our data was estimated as 10 mmag or less, they were retained in the *Gaia* SPSS candidate list. Otherwise, the candidate SPSS were rejected from the list. In all doubtful cases, we made extensive use of the available literature data and of our absolute photometry measurements (that will be published in a forthcoming paper) to reach a decision.

In conclusion, of the 162 monitored SPSS candidates, 150 were validated against short-term variability, and only 12 were rejected: eight were found to be variable stars, and four were classified as suspected variables. Among the confirmed or suspected variable stars, there are some widely used flux standards from the CALSPEC set, i.e. BD+174708, SA 105−448, 1740346, and HD 37725.

ACKNOWLEDGEMENTS

We would like to acknowledge the financial support of the Istituto Nazionale di Astrofisica (INAF) and specifically of the Bologna and Roma Observatories; of ASI (Agenzia Spaziale Italiana) under contract to INAF: ASI 2014-049-R.0 dedicated to ASDC, and under contracts to INAF: ARS/96/77, ARS/98/92, ARS/99/81, I/R/32/00, I/R/117/01, COFIS-OF06-01,ASI I/016/07/0, ASI I/037/08/0, ASI I/058/10/0, ASI 2014-025-R.0, ASI 2014-025-R.1.2015 dedicated to the Italian participation to the *Gaia* Data Analysis and Processing Consortium (DPAC). This work was supported by the MINECO (Spanish Ministry of Economy) – FEDER through grant ESP2014-55996-C2-1-R and MDM-2014-0369 of ICCUB (Unidad de Excelencia 'María de Maeztu'). We acknowledge financial support from the PAPIIT project IN103014.

The survey presented in this paper relies on data obtained at ESO (proposals 182.D-0287, 093.D-0197, 094.D-0258), Calar Alto (proposals H08-2.2-041, H10-2.2-042, F11-2.2-033), TNG (proposals AOT17_3, AOT19_14, AOT20_41, AOT21_1, AOT29_Gaia_013/id7), NOT (proposals 49-013, 50-012), Loiano (15 accepted proposals starting from 2007 June), San Pedro Mártir (seven accepted proposals starting from 2007 October), REM (proposals AOT16_16012, AOT17_17012, AOT18_18002, AOT29_Gaia_013/id10), and TJO (proposal 11010).

We warmly thank the technical staff of the San Pedro Mártir, Calar Alto, Loiano, La Silla NTT and REM, Roque de Los Muchachos TNG and NOT, and Montsec TJO observatories. Based on observations made with the Italian Telescopio Nazionale Galileo (TNG) operated on the island of La Palma by the Fundacin Galileo Galilei of the INAF (Istituto Nazionale di Astrofisica) at the Spanish Observatorio del Roque de los Muchachos of the Instituto de Astrofisica de Canarias. Based on observations made with the Nordic Optical Telescope, operated by the Nordic Optical Telescope Scientific Association at the Observatorio del Roque de los Muchachos, La Palma, Spain, of the Instituto de Astrofisica de Canarias. Based on observations collected at the Observatorio Astronómico Nacional at San Pedro Mártir, B.C., Mexico. We made use of the following softwares and online data bases (in alphabetical order): 2MASS, AAVSO, CALSPEC, Catalina Sky Survey (CSS), CATAPACK, ESO-DSS, IRAF, NSVS, SAOIMAGE DS9, SDSS and SEGUE, SExtractor, SIMBAD, SUPERMONGO and *WISE*. The CSS survey is funded by the National Aeronautics and Space Administration under Grant No. NNG05GF22G issued through the Science Mission Directorate Near-Earth Objects Observations Programme. The CRTS survey is supported by the U.S. National Science Foundation under grants AST-0909182 and AST-1313422. This publication makes use of data products from the *Wide-field Infrared Survey Explorer*, which is a joint project of the University of California, Los Angeles, and the Jet Propulsion Laboratory/California Institute of Technology, funded by the National Aeronautics and Space Administration.

Some of the data presented in this paper were obtained from the Mikulski Archive for Space Telescopes (MAST). STScI is operated by the Association of Universities for Research in Astronomy, Inc., under NASA contract NAS5-26555. Support for MAST for non-HST data is provided by the NASA Office of Space Science via grant NNX09AF08G and by other grants and contracts. This research has made use of the SIMBAD database, operated at CDS, Strasbourg, France.

REFERENCES

Abbas M. A., Grebel E. K., Martin N. F., Burgett W. S., Flewelling H., Wainscoat R. J., 2014, MNRAS, 441, 1230

Downloaded from https://academic.oup.com/mnras/article/462/4/3616/2589704 by guest on 09 April 2021

Altavilla G. et al., 2015, Astron. Nachr., 336, 515 (Paper II)
Althaus L. G., Córsico A. H., Isern J., García-Berro E., 2010, A&AR, 18, 471
Aznar Cuadrado R., Jordan S., Napiwotzki R., Schmid H. M., Solanki S. K., Mathys G., 2004, A&A, 423, 1081
Beers T. C., Allende Prieto C., Wilhelm R., Yanny B., Newberg H., 2004, Publ. Astron. Soc. Aust., 21, 207
Bertin E., Arnouts S., 1996, A&AS, 117, 393
Bohlin R. C., 2007, ASP Conf. Ser. Vol. 364. HST Stellar Standards with 1 per cent Accuracy in Absolute Flux. Astron. Soc. Pac., San Francisco, p. 315
Bohlin R. C., Landolt A. U., 2015, AJ, 149, 122
Bohlin R. C., Colina L., Finley D. S., 1995, AJ, 110, 1316
Castanheira B. G. et al., 2007, A&A, 462, 989
Cutri R. M. et al., 2013, VizieR Online Data Catalog, 2328
Dolez N., Vauclair G., Koester D., 1991, in Vauclair G., Sion E., eds, NATO ASI Ser. C, Vol. 336, White Dwarfs. Kluwer, Dordrecht, p. 361
Drake A. J. et al., 2009, ApJ, 696, 870
Dvorak S. W., 2004, Inf. Bull. Var. Stars, 5542, 1
Eyer L., Grenon M., 1997, Hipparcos - Venice '97. ESA Special Publ., 402, 467
Gianninas A., Bergeron P., Fontaine G., 2005, ApJ, 631, 1100
Giovannini O., Kepler S. O., Kanaan A., Wood A., Claver C. F., Koester D., 1998, Balt Astron., 7, 131
Halbwachs J.-L. et al., 2014, MNRAS, 445, 2371
Herbig G. H., 1999, PASP, 111, 1144
Kaiser M. E. et al., 2014, SPIE, 9143, 91434Y
Kepler S. O., Giovannini O., Kanaan A., Wood M. A., Claver C. F., 1995, Balt. Astron., 4, 157
Kharchenko N. V., Roeser S., 2009, VizieR Online Data Catalog, 1280
Kilkenny D., 2007, Commun. Astroseismol., 150, 234
Klagyivik P. et al., 2016, AJ, 151, 110
Koester D., Voss B., Napiwotzki R., Christlieb N., Homeier D., Lisker T., Reimers D., Heber U., 2009, A&A, 505, 441
La Palombara N., Esposito P., Mereghetti S., Tiengo A., 2014, A&A, 566, A4
Landolt A. U., 1983, AJ, 88, 439
Landolt A. U., Uomoto A. K, 2007, AJ, 133, 768
Latham D. W., Stefanik R. P., Torres G., Davis R. J., Mazeh T., Carney B. W., Laird J. B., Morse J. A., 2002, AJ, 124, 1144
Latour M., Fontaine G., Chayer P., Brassard P., 2013, ApJ, 773, 84
Latour M., Fontaine G., Green E. M., Brassard P., 2015, A&A, 579, A39
Lindegren L., Perryman M. A. C., 1996, A&AS, 116, 579
Marinoni S., 2011, PhDT, Bologna University
Marinoni S., Pancino E., Altavilla G., Cocozza G., Carrasco J. M., Monguió M., Vilardell F., 2012, Gaia Technical Report No. GAIA-C5-TN-OABO-SMR-001
Marinoni S., Galleti S., Cocozza G., Pancino E., Altavilla G., 2013, Gaia Technical Report No. GAIA-C5-TN-OABO-SMR-002
Massey P., Gronwall C., 1990, ApJ, 358, 344
McCook G. P., Sion E. M., 1999, ApJS, 121, 1
McGraw J. T., 1977, PhD thesis
Mignard F., 2005, ASP Conf. Ser. Vol. 338. The Gaia Mission: Science Highlights. Astron. Soc. Pac., San Francisco, p. 15
Nascimbeni V., Bedin L. R., Piotto G., De Marchi F., Rich R. M., 2012, A&A, 541, A144
Pancino E. et al., 2012, MNRAS, 426, 1767 (Paper I)
Stritzinger M., Suntzeff N. B., Hamuy M., Challis P., Demarco R., Germany L., Soderberg A. M., 2005, PASP, 117, 810
Ulla A., Thejll P., 1998, A&AS, 132, 1
Woźniak P. R. et al., 2004, AJ, 127, 2436
Xue X. X. et al., 2008, ApJ, 684, 1143
Yanny B. et al., 2009, AJ, 137, 4377
Zapatero Osorio M. R., Martín E. L., 2004, A&A, 419, 167
Zuckerman B., 2014, ApJ, 791, L27

SUPPORTING INFORMATION

Additional Supporting Information may be found in the online version of this article:

Table 2. Best light curves for the 162 monitored SPSS.
Table 3. Results.
Figure 6. The best light curve for each monitored SPSS candidate is displayed in each panel using the same magnitude scale, when possible (http://www.mnras.oxfordjournals.org/lookup/suppl/doi:10.1093/mnras/stw1886/-/DC1).

Please note: Oxford University Press is not responsible for the content or functionality of any supporting materials supplied by the authors. Any queries (other than missing material) should be directed to the corresponding author for the article.

This paper has been typeset from a TEX/LATEX file prepared by the author.

Downloaded from https://academic.oup.com/mnras/article/462/4/3616/2589704 by guest on 09 April 2021